Numerical simulation of flow alterations after carotid artery stenting from multi-modality image data

J.R. Cebral[a,*], M.A. Castro[a], C.M. Putman[b]

[a]School of Computational Sciences, George Mason University, 4400 University Drive, Fairfax, VA 22030, USA
[b]Interventional Neuroradiology, Inova Fairfax Hospital, Falls Church, VA 22040, USA

Abstract

The alterations in the blood flow pattern in a diseased carotid artery after treatment with a stent were analyzed. Realistic patient-specific computational models were constructed from pre- and post-stenting 3D rotational angiography (3DRA) images. Pre-stenting flow conditions were obtained from phase-contrast magnetic resonance (PC-MR) measurements. Post-stenting flow conditions were estimated from the pre-stenting flows measured on the contralateral side. A sensitivity of the post-stenting results with respect to the prescribed flow conditions was carried out. In this particular patient, the stent reduces the shear stress in the region of the stenosis, but also produces flow disturbances near the proximal end of the stent. This type of simulation can potentially be used to assess the outcome of endovascular interventions.

Keywords: Hemodynamics; Carotid artery; Stenting; Rotational angiography; Magnetic resonance

1. Introduction

Stroke is the leading cause of long-term disability and third cause of death after cancer and heart disease in the western world. Carotid artery atherosclerosis is a major cause of stroke. Carotid artery stenting is being actively explored as a less invasive alternative to the traditional carotid artery endarterectomy [1]. Complications of angioplasty and stenting include cerebral embolism associated with intravascular manipulation, hemodynamic compromise during balloon inflation, vessel dissection, early restenosis or occlusion, cerebral hyperperfusion, and intracranial hemorrhage. Restenosis after carotid stenting remains a major problem limiting the efficacy of the procedure. Even though the mechanisms of in-stent restenosis are not fully understood, stent implantation changes the geometry of the vessel creating new regions of decreased and increased shear stress that might be related to the observed restenosis patterns [2,3,4]. The planning of a stenting procedure and the prevention of complications are done based on the experience of the operator and the long-term outcomes are still not established. Image-based computational hemodynamics is increasingly been used to study genesis and progression of vascular disease, enhance image-based diagnosis and plan surgical and interventional procedures. In this paper, the alterations of the flow dynamics in the carotid artery produced by endovascular treatment of stenotic lesions with stents are analyzed.

2. Methods

A patient-specific model of the diseased right carotid artery was constructed from pre-stenting 3DRA using an iso-surface deformable model [5]. Numerical solutions of the 3D unsteady Navier-Stokes equations were obtained using an implicit finite element formulation [6]. Vessel wall compliance and non-Newtonian blood rheology were neglected. The physiologic flow conditions were derived from PC-MR measurements above and below the carotid bifurcation [7].

A post-treatment vascular model was constructed from 3DRA images taken immediately after the procedure. Post-treatment flow conditions were estimated from pre-stenting flows measured on the contralateral side. In other words, for the post-stenting simulation, the flows in the common and internal carotid arteries

* Corresponding author. Tel.: +1 (703) 993 4078; Fax: +1 (703) 993 4064; E-mail: jcebral@gmu.edu

Computational Fluid and Solid Mechanics 2005
K.J. Bathe (Editor)

were taken from the PC-MR flow measurement of the left side.

In order to assess the influence of the estimated flow conditions on the post-stenting results, a sensitivity analysis was carried out. For this purpose, the post-stenting flows were computed as:

$$Q = (1 - \alpha)Q_l + \alpha Q_r \quad (1)$$

where Q represents the post-stenting flow in the internal or common right carotid artery, Q_l is the pre-stenting flow in the right carotid and Q_r is the pre-stenting flow in the left carotid. The parameter α was set to 0.25, 0.50, 0.75 and 1.0 to obtain a range of flow conditions with increasing mean flow.

3. Results

Figure 1 shows volume renderings of the pre- and post-stenting 3DRA images of the right carotid artery and the corresponding vascular models. The maximum intensity projection (MIP) of a contrast-enhanced magnetic resonance angiography (MRA) and the locations of the PC-MR slice planes are also shown in Fig. 1.

A total of five computational fluid dynamics (CFD) simulations were performed, one on the pre-stenting model and four on the post-stenting vascular model under different flow conditions, as explained before. The post-stenting results were qualitatively in agreement, only the magnitude of hemodynamic variables changed with the different flow conditions, but not the gross characteristics of the flow patterns. For this reason, only the post-stenting results for $\alpha = 0.75$ will be shown.

Visualizations of the distribution of the mean wall shear stress (WSS) magnitude and oscillatory shear index (OSI) were produced, and are presented in Fig. 2. After the deployment of the stent, a significant reduction in the mean WSS in the region of the stenosis is achieved. However, new regions of increased OSI near the proximal end of the stent and below the bifurcation were created.

Animations of the instantaneous velocity magnitude on a cut along the vessel axis were created. Snapshots of these animations are shown in Fig. 3 at different time frames during the cardiac cycle. The pre-stenting images show the high speed jet through the stenosis and a recirculation region in the carotid bulb. The post-stenting images show that the high speed jet in the internal carotid artery was deviated towards the outer wall of the vessel, and that new recirculation regions were created near the proximal end of the stent. This latter observation can be more precisely appreciated in the visualizations presented in Fig. 4. In this case, instantaneous streamlines colored with the velocity magnitude are shown at the same instants of time during the cardiac cycle as in Fig. 3. The flow recirculation regions near the proximal end of the stent and in the carotid bulb are clearly seen.

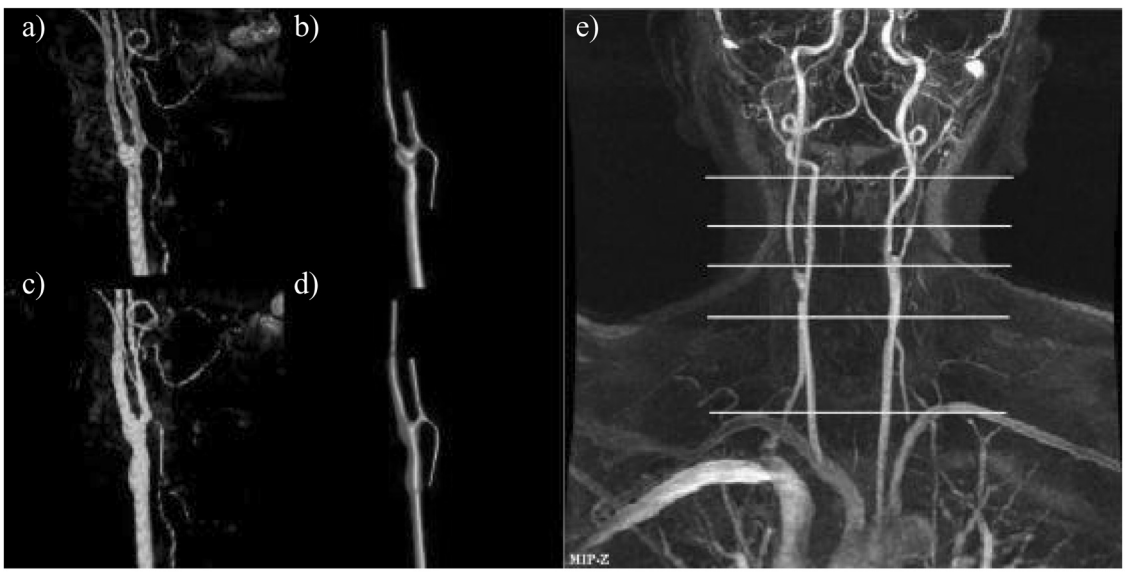

Fig. 1. Image-based vascular models of carotid artery before and after endovascular treatment with stent: (a) volume rendering of the pre-treatment 3DRA image, (b) pre-treatment vascular model, (c) volume rendering of the post-treatment 3DRA image, (d) post-treatment vascular model, and (e) maximum intensity projection of MRA image and location of PC-MR slice planes.

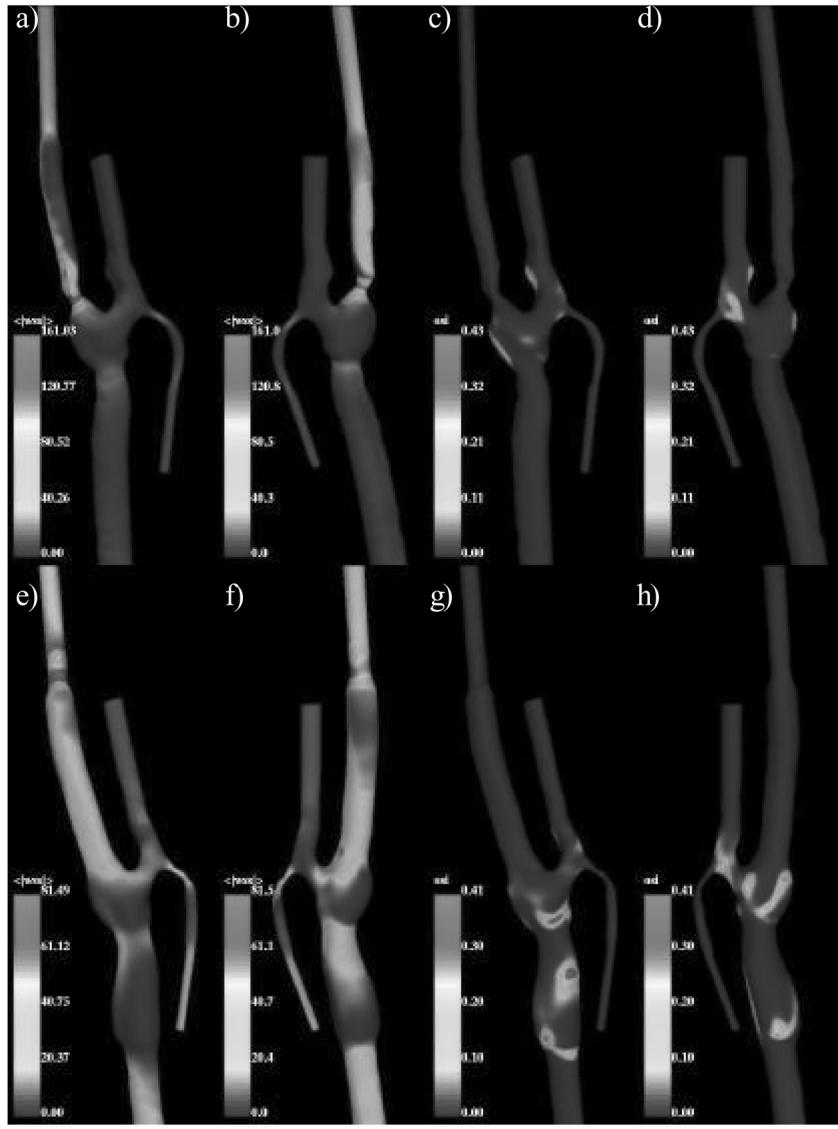

Fig. 2. Visualization of mean wall shear stress (WSS) and oscillatory shear index (OSI) in the pre- and post-stenting models: (a, b) WSS before stenting, (c, d) OSI before stenting, (e, f) WSS after stenting, (g, h) OSI after stenting.

4. Conclusions

In conclusion, patient-specific computational models of the hemodynamics in the carotid artery before and after endovascular treatment with stents can be constructed from multi-modality image data. The simulations presented in this paper showed that the deployment of the stent caused a reduction in the mean wall shear stress in the region of the stenosis, and at the same time produced flow disturbances near the proximal end of the stent. This is due to a slight over-sizing of the stent. The clinical consequences of these alterations in the flow patterns are still unknown. Follow-up studies to correlate the flow characteristics and the clinical outcomes of these endovascular procedures are needed.

Acknowledgments

We thank the Whitaker Foundation for financial support. We also thank Philips Medical Systems and Richard Kemkers for encouragement and technical support.

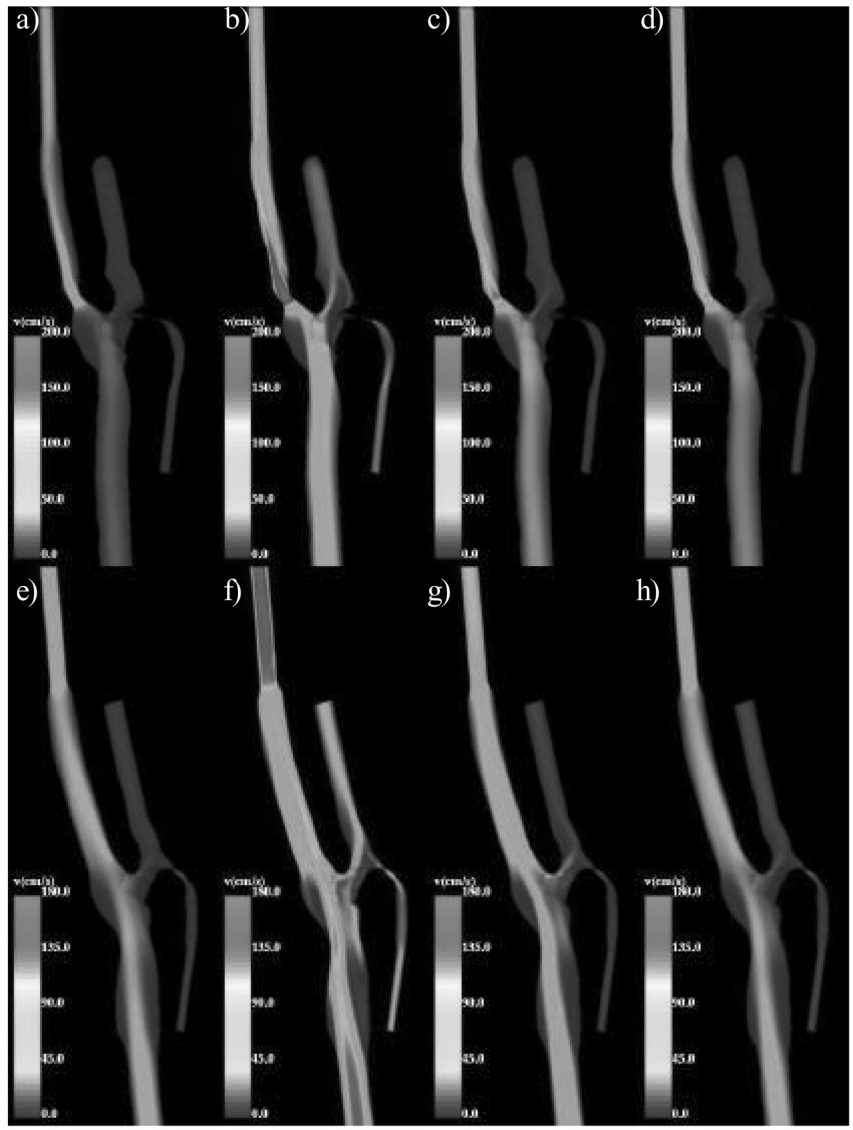

Fig. 3. Visualization of velocity magnitude in a cut along the vessel axis at different instants of time during the cardiac cycle for the pre-stenting model (a–d) and the post-stenting model (e–h).

References

[1] Vitek JJ, Roubin GS, New G, Al-Mubarek N, Iyer SS. Carotid stenting. Techniques Vascular Interventional Radiology 2000;3(2):75–85.

[2] Berger SA, Jou LD. Flow in stenotic blood vessels. Ann Rev Fluid Mech 2000;32:347–382.

[3] Jou LD, Saloner DA. Numerical study of magnetic resonance angiography images for pulsatile flow in the carotid bifurcation. Med Eng Phys 1998;20(9):643–52.

[4] Wentzel JJ, Whelan DM, van Der Giessen WJ, van Beusekom HMM, Andhyiswara I, Serruys PW, Slager CJ, Kram R. Coronary stent implantation changes 3D vessel geometry and 3D shear stress distribution. J Biomech 2000;33:1287–1295.

[5] Yim PJ, Vasbinder B. et al. A deformable isosurface and vascular applications. In: Proc. of SPIE, Vol. 4684 Medical Imaging, San Diego, CA, J.M. Fitzpatrick, editor, Milan: Image Processing 2002, pp. 1390–1397.

[6] Cebral JR, PJ Yim et al. Blood flow modeling in carotid arteries using computational fluid dynamics and magnetic resonance imaging. Academic Radiology 2002;9:1286–1299.

[7] Cebral JR, Castro MA et al. Blood flow models of the circle of Willis from magnetic resonance data. J Eng Math 2003;47(3–4):369–386.

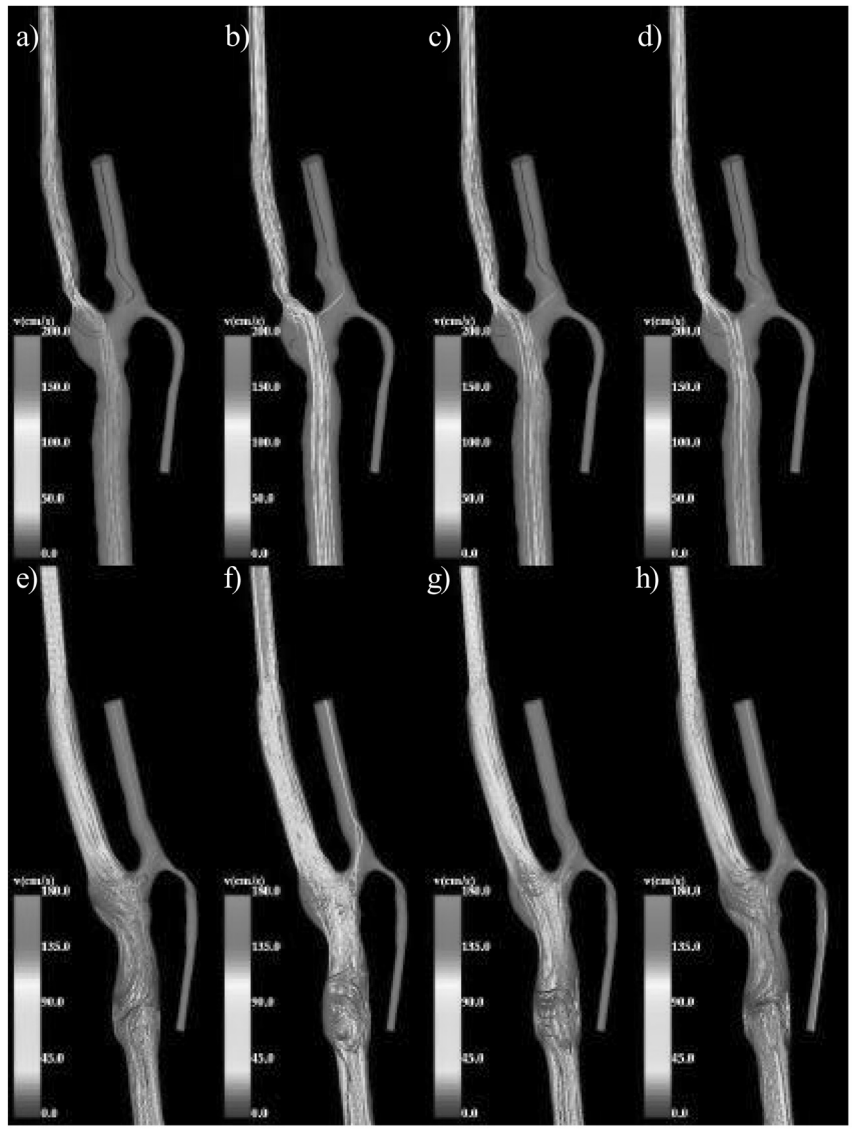

Fig. 4. Visualization of instantaneous streamlines at the same time frames of Fig. 3 for the pre-stenting model (a–d) and the post-stenting model (e–h).